MOLECULAR AND CELLULAR BIOLOGY, Feb. 2011, p. 818–831 Vol. 31, No. 4
0270-7306/11/$12.00 doi:10.1128/MCB.00687-10

Domains of Tra1 Important for Activator Recruitment and Transcription Coactivator Functions of SAGA and NuA4 Complexes▽†

Bruce A. Knutson and Steven Hahn*

Fred Hutchinson Cancer Research Center, Division of Basic Sciences, 1100 Fairview Ave. N., P.O. Box 19024, Mailstop A1-162, Seattle, Washington 98109

Received 14 June 2010/Returned for modification 22 July 2010/Accepted 28 November 2010

The Tra1 protein is a direct transcription activator target that is essential for coactivator function of both the SAGA and NuA4 histone acetyltransferase (HAT) complexes. The ~400-kDa *Saccharomyces cerevisiae* Tra1 polypeptide and its human counterpart TRRAP contain 67 or 68 tandem α-helical HEAT and TPR protein repeats that extend from the N terminus to the conserved yet catalytically inactive phosphatidylinositol 3-kinase (PI3K) domain. We generated a series of mutations spanning the length of the protein and assayed for defects in transcription, coactivator recruitment, and histone acetylation at SAGA- and NuA4-dependent genes. Inviable *TRA1* mutants all showed defects in SAGA and NuA4 complex stability, suggesting that similar surfaces of Tra1 mediate assembly of these two very different coactivator complexes. Nearly all of the viable Tra1 mutants showed transcription defects that fell into one of three classes: (i) defective recruitment to promoters, (ii) reduced stability of the SAGA and NuA4 HAT modules, or (iii) normal recruitment of Tra1-associated subunits but reduced HAT activity *in vivo*. Our results show that Tra1 recruitment at Gcn4-dependent and Rap1-dependent promoters requires the same regions of Tra1 and that separate regions of Tra1 contribute to the HAT activity and stability of the SAGA and NuA4 HAT modules.

Transcription activation of eukaryotic protein coding genes requires one or more sequence-specific DNA binding activators that function in part by recruiting coactivators, chromatin-remodeling factors, and general transcription factors to promoters. In *Saccharomyces cerevisiae*, activators such as Gal4 and Gcn4 target a relatively small number of polypeptides that belong to six coactivator complexes: Spt-Ada-Gcn5-acetyltransferase (SAGA), SAGA-like (SLIK), the histone H4 nucleosomal acetyltransferase (NuA4) complex, TFIID, SWI/SNF, and Mediator (8, 17, 25, 33, 72). One of these direct activator targets is Tra1, an essential 400-kDa protein that is a common subunit of three coactivator complexes: SAGA, SLIK, and NuA4 (3, 32, 70, 76). These Tra1-containing complexes are evolutionarily conserved, and the Tra1 human homolog transformation/transactivation domain-associated protein (TRRAP) is a component of four different coactivator complexes (56), including STAGA (Spt3-TafII31-Gcn5L acetylase), TFTC (TATA-binding protein free), PCAF (p300/CBP-associated factor), and TIP60 (HIV Tat-interacting protein 60). STAGA, TFTC, and PCAF are the mammalian equivalents of SAGA, and the TIP60 complex is the mammalian equivalent of NuA4 (3, 15, 39, 55).

Tra1 is a member of the phosphatidylinositol 3-kinase (PI3K)-related protein kinase (PIKK) protein family, which regulates a diverse set of signaling pathways by serine/threonine phosphorylation (1, 2, 38). Tra1 and its human homolog TRRAP are catalytically inactive since they lack several critical residues necessary for protein phosphorylation, but they retain the structural fold of the PI3K domain (61, 76). TRRAP is a functional target of oncogenic transcription factors that include myc, E2F, and E1a (13, 22, 46, 48). Like Tra1, TRRAP is an essential protein (56, 57, 66), as embryos lacking TRRAP die before implantation, consistent with the results of TRRAP depletion in mammalian cells (19, 34, 35, 89). These studies implicate TRRAP in a broad spectrum of gene regulatory functions that include roles in developmental gene expression and stem cell identity.

Coactivators such as SAGA, TFIID, and Mediator act as intermediates between activators and the general transcription machinery by performing essential functions that facilitate transcription. SAGA is a 1.8-MDa complex composed of 20 subunits that affects the transcription of at least 10% of yeast genes (50). Genome-wide studies in yeast showed that SAGA-dependent promoters are typically highly regulated TATA-containing promoters that are induced by environmental stress (37). SAGA is a multifunctional coactivator complex that contains five different functional modules with roles in nucleosome modification, complex integrity, TATA binding protein (TBP) interaction, deubiquitylation, and activator interaction. Upon gene activation, SAGA is rapidly recruited to promoters where its histone acetyltransferase (HAT) subunit Gcn5 acetylates several lysines of histone H3. Previous studies demonstrated that SAGA has important coactivator functions apart from its HAT activity, since elimination of Gcn5 affects the expression of only a small subset of SAGA-dependent genes (50). One of these critical coactivator functions is to interact with the general transcription machinery. Genetic and cross-linking studies showed that at least two subunits of SAGA directly interact

* Corresponding author. Mailing address: Fred Hutchinson Cancer Research Center, Division of Basic Sciences, 1100 Fairview Ave. N., P.O. Box 19024, Mailstop A1-162, Seattle, WA 98109. Phone: (206) 667-5261. Fax: (206) 667-6497. E-mail: shahn@fhcrc.org.

† Supplemental material for this article may be found at http://mcb.asm.org/.

▽ Published ahead of print on 13 December 2010.

with TBP (49, 54, 60, 79). Interaction of the SAGA subunit Spt3 with TBP is important for transcription activation and leads to recruitment of the transcription machinery to SAGA-regulated promoters. SAGA also contains a ubiquitin protease module that regulates the level of H2B-ubiquitin, a key determinant of histone methylation levels in transcribed regions and transcription elongation (75, 87, 90).

Another Tra1-containing coactivator complex is the SAGA-related complex SLIK, which regulates a distinct set of genes. SLIK is similar to SAGA but contains a truncated version of the Spt7 subunit and has replaced one of the TBP-interacting subunits, Spt8, with Rtg2 (70). Rtg2 is essential for SLIK complex integrity and is one of three RTG genes important for the retrograde response pathway leading to expression of genes in times of metabolic dysfunction (11, 45). The third Tra1-containing coactivator is the 12-subunit NuA4 complex, which contains the essential HAT subunit Esa1. NuA4 preferentially acetylates lysines within histone H4 and, to a lesser extent, histone H2A. Unlike SAGA and SLIK, NuA4 lacks subunits that interact with TBP or other components of the transcription machinery. Therefore, NuA4 functions in gene regulation as an activator-targeted HAT, similarly to mammalian coactivators p300/CBP. Targeted recruitment of NuA4 to gene promoters has been observed for ribosomal protein genes, TATA-less TFIID-regulated genes, and a subset of SAGA-dependent genes (24, 27, 58, 64, 73, 74). NuA4 has also been shown to have an important role in DNA repair and is recruited to double-stranded DNA breaks, where it acetylates histones around damaged sites to promote DNA end joining and repair (10, 23, 85). Recent reports also suggest that NuA4 and SAGA are targeted to coding regions of active genes, where they modify histones in the coding sequence, stimulating transcription elongation (28, 29, 68).

Here we investigate the role of Tra1 in activated transcription. The large size of Tra1 and its strict requirement for cell viability have complicated previous studies of this protein in yeast and human systems. Using a new strategy to detect protein repeats, we predict that Tra1 and TRRAP contain a large tandem array of HEAT and TPR repeats extending from the N terminus to the PI3K domain. We used this prediction to identify regions of Tra1 important for cell viability, SAGA and NuA4 complex integrity, and targeted recruitment by activator. We show that Tra1 acts as an important scaffold for SAGA and NuA4 complexes and that it is also important for a step involving histone acetylation subsequent to Tra1 recruitment.

MATERIALS AND METHODS

Protein repeat and domain analysis and 3D modeling. Protein repeat and domain predictions were conducted as previously described (43). Briefly, structure similarity searches between homologous proteins were performed by HHpred (http://toolkit.tuebingen.mpg.de/hhpred) (81) using the database of HMM domains of known structure from the Protein Data Bank (PDB) database (http://www.pdb.org/pdb/home/home.do) (7). All searches were conducted with the program's default settings and thresholds, and known structural repeat units were located from the three-dimensional (3D) structures deposited in the PDB database. HMM alignment between yeast Tra1 and TRRAP proteins was generated by HHpred using the Tra1 protein sequence as the query and the human genome as the HMM database source. The 3D model of the PI3K domain of Tra1 was created by HHpred and SWISS-MODEL workspace (http://swissmodel.expasy.org/workspace) (78). Structural templates for the PI3K domain were identified by searching the PDB database with HHpred using default parameters. PIR alignments were created from the template structure of human phosphatidylinositol 3-kinase catalytic subunit type 3 (3ihy), which resulted in the highest probability score. Next, PIR alignments were manually converted to FASTA alignments, and 3D models were built with the SWISS-MODEL workspace using the alignment mode. Surface representations of the PI3K domain were created in PyMOL (21).

Plasmid construction. *TRA1* containing 577 bp upstream and 436 bp downstream of the open reading frame (ORF) was cloned between the SacI and SalI sites of vector pRS316 to create pSH689 (*ars cen URA3 TRA1*). *TRA1* was triple Flag tagged at the N terminus using site-directed mutagenesis and cloned via SacI and SalI to vector PRS314 lacking a KpnI site to create plasmid pSH690 (*ARS CEN TRP1* 3×Flag-*TRA1*), and this plasmid was used as the wild-type (WT) *TRA1* plasmid for all studies in this paper. *TRA1* deletions were created in plasmids pSH680 [N-terminal half of *TRA1* in pBluescript SK(+)] or pSH693 [C-terminal half of *TRA1* in pBluescript SK(+)] using site-directed mutagenesis. A glycine-serine-glycine linker was inserted at the junction of all deletions. *TRA1* deletions were then transferred to pSH690 to generate the *ars cen TRP1* 3×Flag-*TRA1* deletion derivatives used for analysis of *TRA1* mutant phenotypes and summarized in Table S1 in the supplemental material.

Yeast strains. All *TRA1* deletion yeast strains used in this study were derived from BY4705 (*MAT*α Δ*ade2*::*hisG his3*Δ*200 leu2*Δ*0*) (14). The *TRA1* gene was disrupted in this yeast strain by PCR amplifying the *kanMX* gene locus from the pFA6-KanMX4 vector with primers flanking the *TRA1* open reading frame (ORF) to create the following yeast strain: SHY785 [*MAT*α Δ*ade2*::*hisG his3*Δ*200 leu2*Δ*0 lys2*Δ*0 met15*Δ*0 trp1*Δ*63 ura3*Δ*0 TRA1*Δ::*kanMX*(*ARS CEN URA3 TRA1*)]. Additional yeast strains used in this study are as follows: BKY5 (SHY785, *EAF1-TAP*::*hphB*), BKY6 (SHY785, *SPT7-TAP*::*hphB*), BKY7 (SHY785, *GCN5-13myc*::*HIS3*), BKY8 (SHY785, *ESA1-3HA*::*HIS3*) (SHY555, *MAT*α Δ*ade2*::*hisG his3*Δ*200 leu2*Δ*0 lys2*Δ*0 met15*Δ*0 trp1*Δ*63 ura3*Δ*0 SPT7*-3×Flag::*kanMX*), BKY9 (SHY555, *spt20*Δ::*hphB*), W1588-4C (*MAT***a** *ade2-1 can1-100 his3-11,15 leu2-3,112 trp1-1 ura3-1 RAD5*$^+$), YTT2256 (W1588-4C, *YNG2*Δ::*natMX*) (53), YTT2329 (W1588-4C, *EAF1*Δ::*natMX*) (53), SHY787 (BY4705, *GCN5*Δ::*hphB*), and MSY2431 (*MAT***a** *ade2-1 leu2-3 his3-11 trp1-11 ura3-1 ESA1-1851*::*ura3*) (51).

Growth conditions. For induction of the Gal4-dependent genes, cells were grown in glucose complete (GC) medium lacking tryptophan with 2% raffinose as a carbon source and induced with 2% galactose for 1 h. For induction of Gcn4-dependent genes, cells were grown in GC lacking tryptophan, isoleucine, and valine with 2% glucose as a carbon source and induced with 0.5 μg/ml sulfometuron methyl (SMM) in dimethyl sulfoxide (DMSO) for 1 h before samples were taken. To analyze ribosomal protein gene expression, cells were grown in YPD medium (1% yeast extract, 2% peptone, 2% glucose) supplemented with 0.004% adenine sulfate. Yeast cell viability assays were performed on glucose complete plates containing 1 g/liter 5-fluoroorotic acid (5-FOA). Spot test assays were used to examine growth under different stress conditions. SMM phenotypes were monitored by 5-fold serial dilutions of the isogenic wild type and *TRA1* deletion mutants spotted on GC medium lacking isoleucine, valine, leucine, and tryptophan without drug or with 3.0 μg/ml SMM. Plates without drug were grown for 2 days at 30°C, and SMM-containing plates were grown for 6 days at 30°C. To examine temperature-sensitive phenotypes, serial dilutions were spotted on glucose complete medium lacking tryptophan and grown for 2 days at 24°C, 30°C, and 37°C. To examine galactose-sensitive phenotypes, the wild type and the indicted Tra1 deletion mutants were first grown in complete medium containing 2% raffinose as a carbon source and lacking tryptophan. These cells were washed in water, and then 5-fold serial dilutions were spotted onto complete medium containing 2% galactose and lacking tryptophan and grown for 3 days at 30°C. Yeast growth was assessed by colony size relative to the wild type (WT) (++++).

Immunoprecipitations. Flag-tagged Tra1 was purified from 200-ml mid-log-phase cultures grown in GC lacking tryptophan and uracil. Cells were collected by centrifugation and lysed by bead beating in lysis buffer (100 mM Tris-HCl, pH 7.9, 250 mM $AmSO_4$, 1 mM EDTA, 10% glycerol) supplemented with 0.5 mM dithiothreitol (DTT), 0.5 mM phenylmethylsulfonyl fluoride (PMSF), and EDTA-free complete protease inhibitor cocktail (Roche), and lysates were cleared by centrifugation. Approximately 2 mg of the whole-cell extract diluted with 2 volumes of dilution buffer (25 mM HEPES, pH 7.5, 50 mM NaCl, 1 mM EDTA) was incubated overnight at 4°C with either 30 μl of M2 affinity agarose (Sigma) or 30 μl of anti-c-Myc affinity agarose (Sigma) for Flag or Myc immunoprecipitations, respectively. Beads were washed 3 times in 1 ml 1× Tris-buffered saline (TBS) with 0.1% Tween and 2 times with 1× TBS, and proteins were eluted twice with 2 bead volumes of 1× TBS containing either 350 μg/ml Flag peptide (Sigma), Myc peptide (Sigma), or HA peptide (Sigma). Samples were resolved on 4 to 12% polyacrylamide gradient gels (Invitrogen) in 1× MOPs buffer (50 mM morpholinepropanesulfonic acid [MOPS], 50 mM Tris

base, pH 7.7, 3.5 mM SDS, 1 mM EDTA) for 50 min at 200 V. Proteins were transferred to polyvinylidene difluoride (PVDF) and probed with rabbit polyclonal antibodies against Spt3, Ada1, Taf12, and Esa1; mouse monoclonal antibodies against Yaf9 (Abcam; ab4468), Flag (Sigma), and Myc (Covance; MMS-150R); and goat polyclonal antibodies against Ada2 (SCBT; sc-6651), Ada3 (SCBT; sc-6652), or Gcn5 (SCBT; sc-6305).

ChIP. Chromatin immunoprecipitation (ChIP) assays were conducted as previously described (33, 62, 63) with a few modifications. Briefly, cell cultures were grown to an optical density at 600 nm of 0.5 to 0.8 in GC medium lacking isoleucine, valine, and tryptophan with 2% glucose or GC medium lacking tryptophan with 2% raffinose at 30°C. Cells were induced with 0.5 μg/ml SM or 2% galactose for 1 h and cross-linked with 1% formaldehyde (Sigma) for 15 min at room temperature. After cross-linking, cells were harvested and washed twice with cold 1× TBS buffer. Cells were resuspended in ChIP buffer (150 mM NaCl, 50 mM Tris-HCl, pH 7.5, 5 mM EDTA, 0.5% NP-40, 1.0% Triton X-100) supplemented with 0.5 mM DTT, 0.5 mM PMSF, and EDTA-free complete protease inhibitor cocktail (Roche). Cells were lysed with 0.5-mm zirconia beads (Biospec) using a Mini-Beadbeater-96 (Biospec) at 3-min intervals until greater than 95% cell breakage was achieved. Lysates were sonicated four times for 10 min each on a high setting with the Bioruptor UCD-200 (Diagencode). Sonicated lysates were cleared by centrifugation, and protein concentrations were determined by the Bradford assay. For immunoprecipitations, 1 mg of sheared chromatin was incubated overnight at 4°C with either 2 μg of HA antibody (SCBT; sc-7392), 2 μg of Flag M2 antibody (Sigma; F1804), 2 μg of 9E10 C-Myc antibody (Covance; MMS-150), 2 μg of Rap1 antibody (SCBT; sc-6663), 4 μg of Gcn4 antibody and 2 μg of Gal4 antibody (Abcam; ab1396), 2 μg of Rpb1 antibody (Abcam; 8WG16), 1 μg of H4K8Ac antibody (Millipore; 07-328), 1 μg of H3K9Ac antibody (Millipore; 07-352), or 1 μg of histone H3 antibody (Cell Signaling Technologies; 9712). For ChIPs of C-terminally TAP-tagged Eaf1 and Spt7 proteins, 20 μl of IgG-conjugated Sepharose 6 Fast Flow beads (GE Healthcare) and 2 mg of chromatin were used. Antibody-protein complexes were recovered with 15 μl protein G Dynabeads (Dynal), and beads were washed four times in ChIP buffer containing 500 mM NaCl and once with standard ChIP buffer. Next, 100 μl of 10% Chelex-100 (Bio-Rad) was added to beads and boiled for 10 min. The suspension was centrifuged, and supernatant containing the eluted DNA was collected. The beads were washed with 100 μl water and centrifuged, and the supernatants were combined. Eluted DNA was used directly in PCR. To determine percent wild-type immunoprecipitated ChIP signal, values were calculated as the ratio of the percent precipitated at a specific locus to the percent precipitated at the *POL1* reference locus. All values are expressed relative to the wild-type value, set at 1.0. Experiments were performed in biological triplicate.

GST pulldown assay. Recombinant glutathione *S*-transferase (GST) and GST-Gcn4 1–134 fusion proteins were expressed by autoinduction in ZY5052 medium (25 mM Na_2HPO_4, 25 mM KH_2PO4, 50 mM NH_4Cl, 5 mM Na_2SO_4, 2 mM $MgSO_4$, 0.5% glycerol, 0.05% glucose, 0. 2% α-lactose, 0.01% tryptone, 0.005% yeast extract) for 16 h at 37°C (84). Cells were harvested by centrifugation and washed with 1× phosphate-buffered saline (PBS) buffer (150 mM NaCl, 15 mM $NaPO_4$, pH 7.4) supplemented with 5 mM DTT, 0.5 mM PMSF, and EDTA-free complete protease inhibitor cocktail (Roche). Cells were lysed with 1 mg/ml lysozyme (Sigma) for 30 min on ice followed by sonication. To aid protein solubility and purification, 0.25% Sarkosyl and 2% Triton X-100 were added to the lysates (26). Lysates were cleared by centrifugation, and clear lysates were added to glutathione beads (GE Healthcare) and mixed for 4 h at 4°C. Beads were washed three times with 1× PBS, twice with 1× PBS with 3 M NaCl, and three times with 1× TBS buffer. GST fusion protein was eluted with 3 bead volumes of GST elution buffer (50 mM Tris-HCl, pH 8.0, 10 mM glutathione). Eluted protein was dialyzed in GST pulldown buffer (25 mM Tris-HCl, pH 7.5, 50 mM KCl, 5 mM $MgCl_2$, 0.1% Triton X-100, 2 mM DTT, 10% glycerol) supplemented with protease inhibitor cocktail (Roche). Equivalent amounts of GST fusion protein were bound to magnetic GST beads (Pierce) and blocked with 1% bovine serum albumin (BSA) in GST pulldown buffer. Flag-Tra1-containing SAGA and NuA4 complexes were purified as described above, and equivalent amounts of Flag-Tra1 were added to the blocked GST beads for 2 h at 4°C. Beads were washed five times in GST pulldown buffer, and precipitated proteins were eluted in 1× lithium dodecyl sulfate (LDS) sample buffer and resolved on 4 to 12% polyacrylamide gradient gels (Invitrogen) in 1× MOPs buffer. Proteins were transferred to PVDF and probed with Flag M2 antibody (Sigma) and GST antibody (SCBT; sc-459).

***In vitro* HAT assay.** Histone acetyltransferase (HAT) assays were adapted from references 31 and 47. Equivalent amounts of Flag-Tra1 complexes purified as described above were added to 50-μl reaction mixtures containing 2.5 μg of recombinant histone H3 and 10 μM acetyl coenzyme A (acetyl-CoA) (Sigma) in HAT assay buffer (50 mM Tris-Cl, pH 8.0, 50 mM KCl, 5% glycerol, 0.2 mM EDTA, 2 mM DTT, 20 mM sodium butyrate, 2 mM PMSF). Reaction mixtures were incubated at 30°C for 30 min followed by addition of 1× LDS sample buffer and separation on a 4 to 12% polyacrylamide gradient gel (Invitrogen) in 1× MOPS buffer. Proteins were transferred to PVDF, and acetylated histone H3 was detected using an antibody against H3K9Ac. Total histone H3 levels in each reaction mixture were detected by Coomassie blue staining.

Total RNA isolation. Approximately 10 ml of yeast cells grown to an optical density at 600 nm of 0.6 to 0.8 was pelleted by centrifugation and washed in cold nuclease-free water (Ambion). Cells were resuspended in TES buffer (10 mM Tris, pH 7.5, 10 mM EDTA, 0.5% SDS) and an equal volume of acid phenol (Ambion). The suspension was incubated at 65°C for 1 h, followed by a second acid phenol extraction and a single chloroform (Sigma) extraction. Extracted RNA was ethanol precipitated with sodium acetate and pelleted by centrifugation. RNA pellets were washed with 80% ethanol, air dried, and resuspended in RNase-free water. Next, 15 μg of RNA was treated with the Turbo DNase kit (Ambion) and 1 μg of DNA-free RNA was synthesized into cDNA using Superscript III (Invitrogen) using oligo$(dT)_{20}$ primer according to the manufacturer's instructions. cDNA was diluted 1:100 before quantitative PCR (qPCR) was performed.

Quantitative PCR. Gene-specific qPCR was performed in triplicate using primers near the 3′ end of the gene. Promoter-specific qPCR was also performed in triplicate using primers spanning the upstream activating sequence (UAS) or near the transcription start site (ATG). UAS primer sets were used for activator and Flag-Tra1 ChIPs, and ATG primer sets were used for all other ChIPs. Reverse transcription-qPCR (RT-qPCR) and ChIP primer sequences used in this study are listed in Table S4 in the supplemental material. Primers were designed with either PrimerQuest (IDT) or Primer Express 3 (ABI) software using default parameters. qPCRs were assembled in 5-μl reaction mixtures in a 384-well plate format using an ABI 7900HT sequence detection system for real-time PCR (ABI) and Power SYBR green master mix (ABI). Relative amounts of DNA were calculated using a standard curve generated from a 10-fold serial dilution series of purified yeast genomic DNA ranging from 10 to 0.001 ng DNA. Relative amounts were normalized to *ACT1* for RNA expression analysis and were normalized to *POL1* for ChIP analysis. All values are expressed relative to the wild-type value, set at 1, and error bars denote standard deviations of triplicate and duplicate experiments where indicated.

RESULTS

Sequence analysis of Tra1 and TRRAP. A major obstacle that has impeded structural and functional studies of Tra1 and its human homolog TRRAP is their large size (~430 kDa). The predicted domain structure of Tra1 is well conserved and is similar to those of other members of the PIKK protein family (Fig. 1A) (1, 43, 86). PIKK family members consist of five distinct domains, including a C-terminal PI3K catalytic domain that is inactive in Tra1/TRRAP. Four different α-helical domains flank the PI3K domain. Immediately adjacent to the PI3K domain is a four-helix bundle called the FRB domain (FKBP12 rapamycin binding) and an extended helical region called the FAT domain (FRAP, ATM, and TRRAP) (12, 52). The FAT domain is predicted to form both HEAT (Huntingtin, elongation factor 3, PR65/A, and TOR) and TPR (tetratricopeptide) repeats (4, 16, 42, 69). The C terminus of PIKK proteins contains a FATC domain (FAT C-terminal) composed of one short and one long helix that are joined by a disulfide bond (20). However, one or both of these cysteines are missing in Tra1/TRRAP (36). Finally, the HEAT domain folds into a number of α-helical HEAT repeats that extend from the N terminus to the FAT domain, representing more than half the length of the protein.

Web-based repeat and domain prediction methods, including Pfam, Prosite, SMART, REP, ARD, TPRpred, and HHrepID (5, 9, 42, 65, 77, 80, 82), predicted few or no HEAT and TPR repeats in Tra1/TRRAP. To identify these repeats,

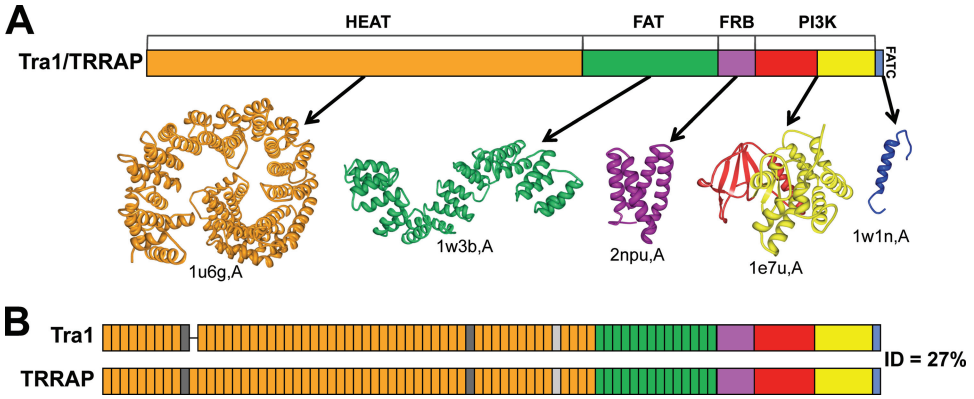

FIG. 1. Comparison of Tra1 and TRRAP domains. (A) Modular structure of the Tra1/TRRAP protein. A representative three-dimensional protein structure for each of the five domains is depicted below each arrow with the corresponding Protein Data Bank code. (B) Alignment of predicted domain and repeat architectures of Tra1 and TRRAP. Individual rectangles in the HEAT and FAT domains represent single HEAT and TPR repeats, respectively. Dark gray rectangles represent predicted disordered regions, and light gray rectangles denote a non-repeat-containing segment. Gaps in the alignment are indicated by a line. ID, identity.

we used a prediction strategy recently developed to detect divergent HEAT and TPR motifs that are missed by conventional methods (43). This approach uses profile-HMM (hidden Markov model) comparisons from the HHpred program to find structural relationships between a protein of interest and proteins with known tertiary structures and has been particularly useful for predicting protein repeats in PIKK protein family members (43, 81). Using the HHpred approach, we detected 67 or 68 protein repeats in Tra1 and TRRAP (Fig. 1B). For Tra1, we predicted a nearly tandem array of 53 HEAT repeats extending from the N terminus up to the boundary of the FAT domain. A nearly identical configuration of 54 HEAT repeats was predicted for TRRAP, with the exception of one additional HEAT repeat. Repeat predictions in the FAT domain of Tra1/TRRAP suggest that this domain is composed of 14 TPR repeats, consistent with previous reports for other PIKK protein family members (16, 43).

Although Tra1 and TRRAP share a modest 27% amino acid sequence identity, their predicted secondary structures are remarkably similar, and repeat analysis revealed that approximately 98% of the predicted helical repeats aligned well between the two proteins when their protein sequences were compared (see Fig. S1 in the supplemental material) (18). The Tra1 HEAT domain contains a tandem array of repeats that are interrupted by two predicted disordered regions between HEAT repeats 9 and 10 and HEAT repeats 40 and 41. Disordered regions are also predicted in nearly identical positions of TRRAP, the first between HEAT repeats 9 and 10, which corresponds to a repeated proline stretch, and the second between HEAT repeats 41 and 42. The FRB, PI3K, and FATC domains of Tra1 and TRRAP are also conserved at the sequence level and are predicted to have nearly identical tertiary structures. These observations suggest that Tra1 and TRRAP have similar structures and provide a framework to test the importance of these conserved domains.

Regions of Tra1 important for cell viability. To identify functional domains within Tra1, we constructed a series of 44 internal deletions spanning the entire length of the protein using the above repeat and domain prediction as a guide. Each deletion removed ~100 amino acid residues (Fig. 2A). Deletions in the HEAT and TPR domains were specifically designed to remove 1 to 3 repeat units. Since Tra1 is essential for viability, we transformed these mutant constructs into a *tra1*Δ strain carrying the wild-type *TRA1* locus on a *URA3*-marked plasmid, and transformants were plated on 5-fluoroorotic acid (5-FOA). Approximately two-thirds of the *TRA1* mutants were inviable, and many of the remaining viable mutants exhibited slow- and/or temperature-sensitive-growth phenotypes (see Table S1 in the supplemental material).

Lethal *TRA1* mutants were found in each of the five domains (Fig. 2A, red). The FRB, PI3K, and FATC domains were all essential for viability. A single deletion at the junction of the PI3K C-terminal lobe and FATC domain gave rise to viable yeast, whereas a complete deletion of the FATC domain was inviable, possibly due to poor protein stability, since this deletion resulted in a truncation in the C terminus (see below). This is consistent with a previous study suggesting that the FATC domain is important for integrity of complexes containing members of the PIKK protein family (36, 41). We also found that Tra1 regions spanning HEAT repeats 8 and 9, 10 to 25, 20 to 35, and 46 to 53 and TPR repeats 1 to 6 and 10 to 14 were essential for viability. The remaining Tra1 HEAT and TPR repeats, as well as the two aforementioned disordered regions between HEAT repeats 9 and 10 and repeats 40 and 41, were not essential for growth.

A subset of the viable mutants exhibited growth sensitivities consistent with defects in transcription activation (Fig. 3; see also Table S2 in the supplemental material). We examined the effects of three stress conditions on growth of these mutant strains including growth on galactose, sensitivity to temperature (37°C), or sulfometuron methyl (SMM). Of the 15 viable mutants, 12 were moderately sensitive to growth at 37°C. These mutants contained deletions in either the HEAT or FAT domains or at the junction between the PI3K C-terminal lobe and FATC domain. Cell growth in the presence of SMM, an inhibitor of amino acid biosynthesis that requires the activation of Gcn4-dependent genes, was impaired for 12 of 14 mutants. Nearly all of these strains also displayed temperature-sensitive phenotypes, suggesting that these Tra1 mutants may cause a defect in heat stress-induced transcription. We ob-

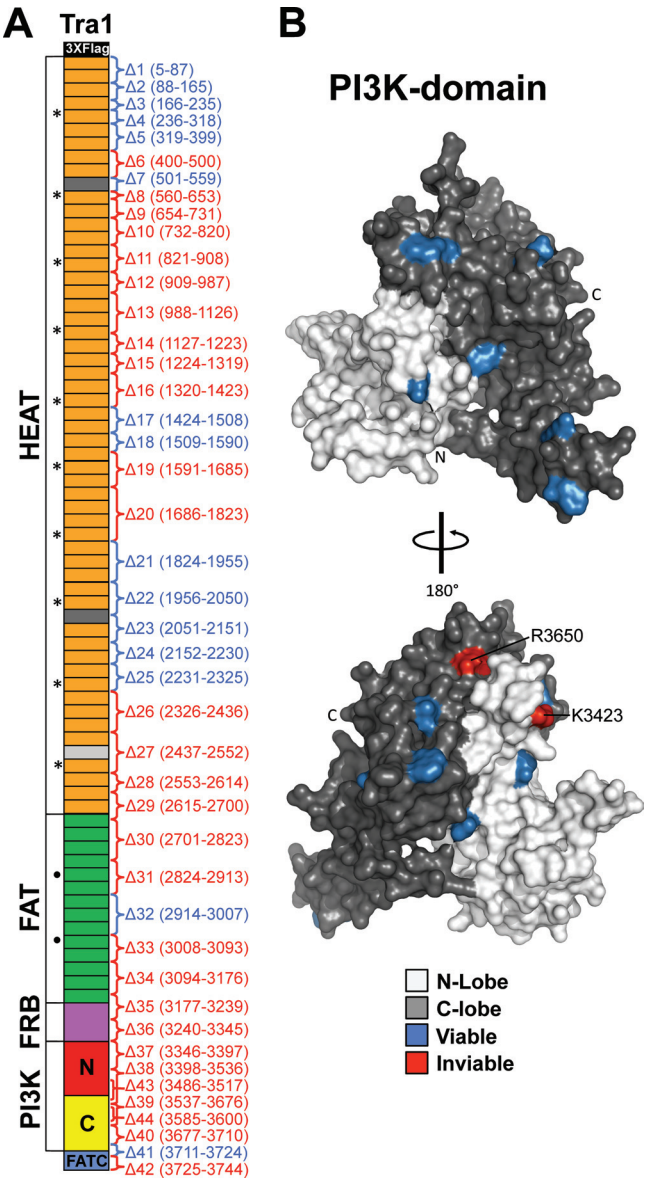

FIG. 2. Summary of *TRA1* deletions and single-amino-acid substitutions in the PI3K domain and their roles in SAGA and NuA4 coactivator function. (A) Schematic of the repeat and domain architecture of Tra1. The color scheme and structural features are the same as in Fig. 1. The deletion name and location are indicated to the left of each bracket. Inviable Tra1 deletions (all causing both SAGA and NuA4 complex integrity defects) are indicated by red lettering, and viable deletions are indicated by blue lettering. Every fifth repeat is denoted by an asterisk or dot in the HEAT and FAT domains, respectively. (B) Surface representation of the PI3K domain of Tra1 based on the crystal structure of 3ihy. The N-terminal and C-terminal lobes of the Tra1 PI3K domain model are colored in white and gray, respectively. Inviable amino acid substitutions are colored red, and viable substitutions are blue.

served poor growth on galactose for only 2 out of the 14 viable mutants (e.g., Δ24 and Δ32), suggesting that the Gal4 and Gcn4 activators may interact differently with Tra1. Finally, we tested the dominance of the *TRA1* deletion mutants when coexpressed with wild-type *TRA1* and observed no significant

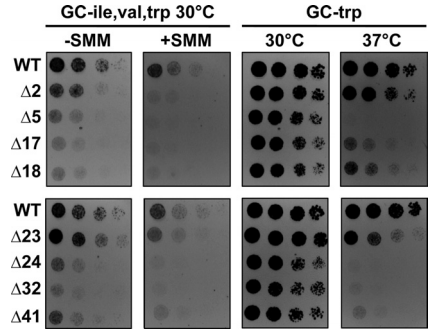

FIG. 3. Growth phenotypes of selected *TRA1* deletion mutants. (Left panels) Viable *TRA1* mutants from Table S1 in the supplemental material were compared with a wild-type strain for growth on glucose complete (GC) medium lacking tryptophan, isoleucine, and valine incubated at 30°C with or without 3 μg/ml SMM. (Right panels) The indicated Tra1 mutations were incubated on GC medium and grown at the indicated temperatures. Fivefold serial dilutions of cells were spotted onto plates.

growth phenotypes under the any of the conditions tested (see Fig. S2 and Table S1).

We also analyzed the function of the PI3K domain by modeling the structure of this domain and mutating predicted surface residues (Fig. 2B). A total of 16 single glutamate substitutions were created, 4 in the N-terminal lobe and 12 in the C-terminal lobe of the PI3K domain. Only two of these mutations, R3432E and R3650E, gave rise to inviable yeast, while the remaining *TRA1* PI3K mutants were viable and grew at or near wild-type levels (see Table S3 in the supplemental material). The two inviable substitutions lie very close together when mapped onto a 3D homology model of the PI3K domain, indicating that these residues form an important interaction interface in this region (Fig. 2B, red). None of the viable PI3K domain mutants displayed sensitivity to temperature, SMM, or galactose (Table S2). From this analysis, we conclude that the PI3K domain is essential but contains few regions participating in functional protein contacts.

Regions of Tra1 important for coactivator complex association. Previous biochemical and genetic studies suggest that Tra1 acts as a molecular scaffold for SAGA and NuA4 complexes (3, 32). To probe this function of Tra1, we tested the panel of Tra1 deletions for association with SAGA and NuA4 subunits. Yeast strains containing both untagged wild-type *TRA1* and Flag-tagged mutant *TRA1* were used to test the ability of the viable and inviable Tra1 mutants to associate with other SAGA and NuA4 subunits by coimmunoprecipitation assays. Western analysis of immunoprecipitated Flag-Tra1 revealed that all Tra1 mutants were expressed at levels ranging from 25% to 100% of wild-type levels. Three inviable *TRA1* deletion mutants gave rise to truncations at or near the site of the deletion (deletions Δ8, Δ39, and Δ42) (Fig. 4; Δ8 is much smaller than wild-type Tra1 and is not shown in the figure). Probing the Western blots for factors coprecipitating with Tra1 surprisingly revealed that all of the inviable Tra1 mutants failed to associate with SAGA subunits Ada1, Spt3, Taf12, and Gcn5 or with NuA4 subunits Esa1 and Yaf9 (Fig. 4). Ada1 and Taf12 are important for SAGA integrity, while the other SAGA subunits assayed (Gcn5 and Spt3) are peripheral sub-

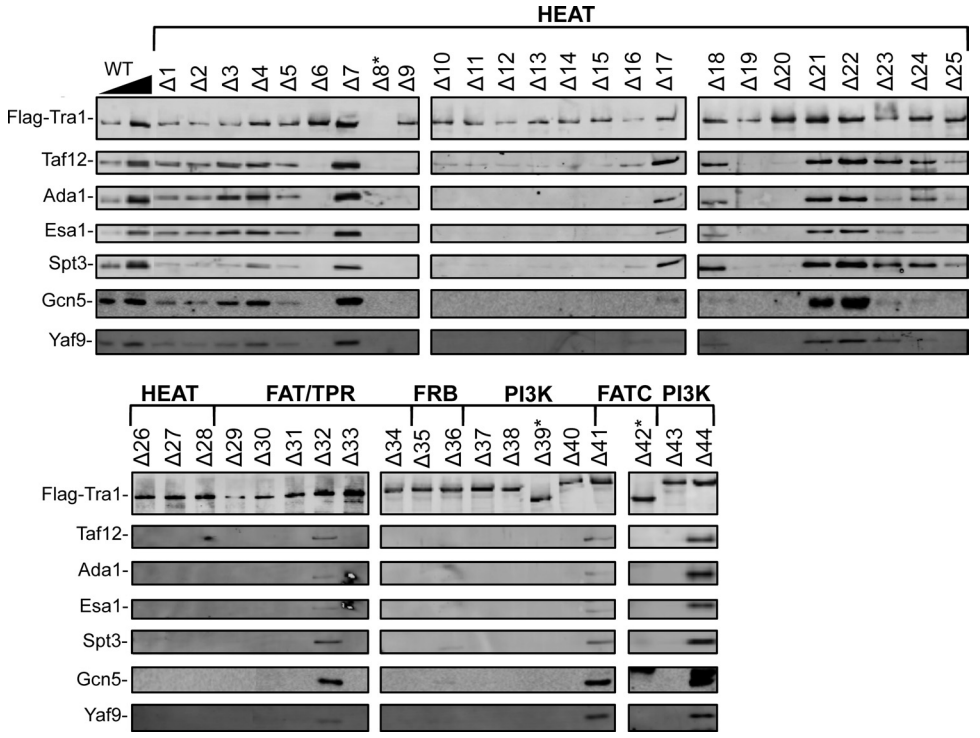

FIG. 4. Effect of *TRA1* mutations on SAGA and NuA4 complex integrity. Western analysis of immunopurified Flag-Tra1. Flag-Tra1 complexes were purified from whole-cell extract and analyzed by Western blotting using the following antibodies: Flag, Ada1, Spt3, Gcn5, Taf12, Esa1, and Yaf9. Tra1 deletions that give rise to a truncated protein are indicted by an asterisk (Δ8 is significantly smaller than wild-type Tra1 and is not visible on this blot).

units (83, 88). The Esa1 and Yaf9 subunits are components of separate functional modules of NuA4 (6, 59). Even though the bulk of Tra1 is composed of multiple repeat units, these repeats are not functionally equivalent, as deletion of only some repeats results in complex instability. It is clear from these results that yeast cell viability is closely linked to the ability of Tra1 to associate with SAGA and NuA4 and that identical regions of Tra1 are required for association with both complexes.

Regions of Tra1 important for transcription activation. Several of the viable *TRA1* mutants form relatively normal levels of SAGA and NuA4 complexes but display strong growth phenotypes, suggesting that they may be defective in coactivator function. To test this, we used quantitative RT-PCR to measure the mRNA levels of three different classes of genes that are activated by activators Rap1, Gcn4, and Gal4 and coactivators SAGA and NuA4. Examining the different activator and coactivator dependencies is necessary to differentiate between activator-specific, coactivator-specific, and general defects in interaction with the transcription machinery subsequent to Tra1 recruitment.

To study defects in Rap1/NuA4-dependent transcription, we measured transcription levels of three ribosomal protein genes, *RPS5*, *RPL2B*, and *RPL11B*. Each of these promoters is dependent on NuA4, as shown by their sensitivities to deletions of NuA4 components but not to disruption of SAGA. For example, deletion of NuA4 subunit *EAF1* or *YNG2* reduced RNA levels by 60 to 70% for each of the ribosomal protein genes examined (Fig. 5A). In contrast, these mRNA levels remain relatively unchanged when the SAGA core subunit *SPT20* is deleted. Our results are consistent with previous findings that transcription of these ribosomal protein genes is dependent on NuA4 but relatively independent of SAGA (58, 73). Seven of the viable *TRA1* mutants showed decreased ribosomal protein transcription levels ranging from 20 to 75% of the wild-type value (deletions Δ2, Δ5, Δ17, Δ23, Δ24, Δ32, and Δ41) (Fig. 6A to C). Tra1 deletion mutants Δ17 and Δ32 showed the most severe reduction in ribosomal protein gene transcription, evidenced by a more than 75% reduction in mRNA levels.

Failure of some Tra1 mutants to stimulate activated transcription could reflect an impaired step downstream of coactivator recruitment or a defect in interaction with activator. To examine the basis for the transcription defects, we used ChIP to measure the recruitment of polymerase II (Pol II) and the Rap1 activator to the *RPL2B* promoter. For all seven of the *TRA1* deletion mutants tested, Rap1 cross-linking levels were relatively unaffected, and Pol II cross-linking correlated well with transcription levels, suggesting that transcription defects were not the result of reduced activator binding or postinitiation defects (Fig. 7A and B). These results suggested that either coactivator recruitment or postcoactivator recruitment steps are defective in these *TRA1* mutants. To differentiate between these models, we measured the levels of the NuA4 subunits Tra1 and Eaf1 cross-linked to the *RPL2B* promoter in these strains (Fig. 7C and D). Three *TRA1* mutants showed decreased cross-linking of Eaf1 and Tra1 at the promoter (Δ2, Δ5, and Δ17), while three other *TRA1* mutants showed near-

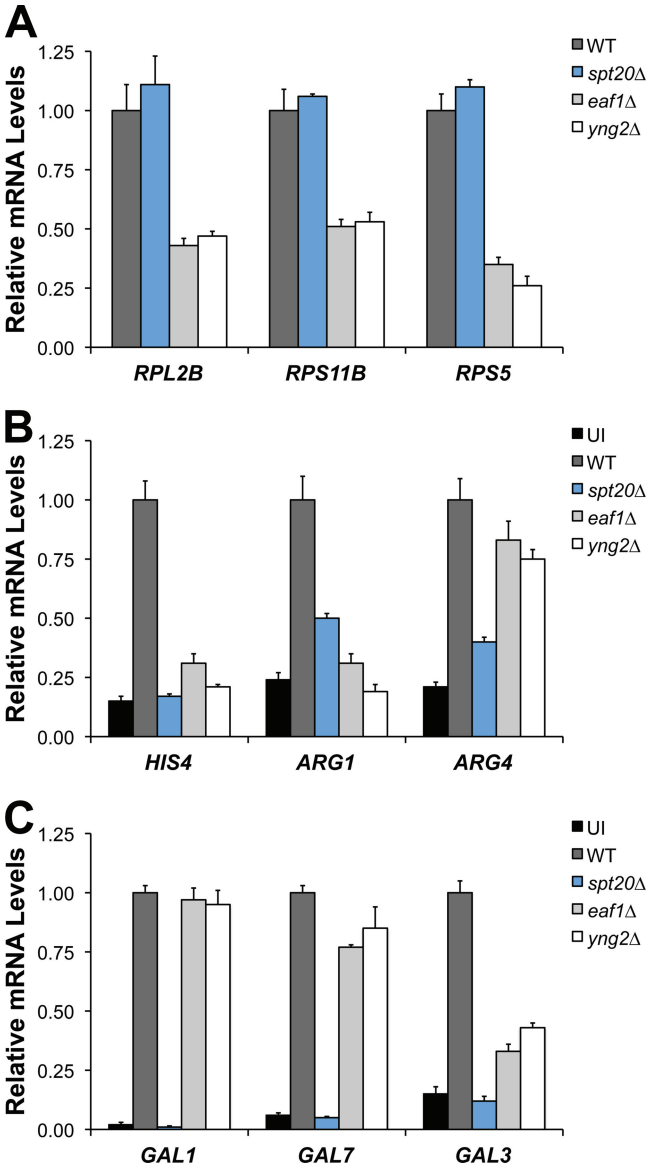

FIG. 5. Effect of SAGA and NuA4 mutations on transcription. Strains containing either wild type (WT) or the indicated SAGA or NuA4 subunit deletions were grown under conditions that induce Rap1-dependent genes (A), Gcn4-dependent genes (B), or Gal4-dependent genes (C). Total cellular RNA was prepared and quantitated by RT-qPCR, and results are represented relative to the wild-type value set at 1.0. UI, not induced. Experiments were performed in biological duplicate, and error bars represent standard deviations.

wild-type cross-linking (Δ24, Δ32, and Δ41). Taken together, these results suggest that transcription defects caused by *TRA1* deletion mutants Δ2, Δ5, and Δ17 are due to reduced recruitment of NuA4 by activator, possibly due to impaired Tra1 interaction. In contrast, transcription defects in *TRA1* mutants Δ24, Δ32, and Δ41 are likely due to postrecruitment defects.

We next tested three Gcn4-activated genes: *HIS4*, *ARG1*, and *ARG4*. Each of these genes is SAGA dependent, as revealed by reduced levels of induced transcription in the *SPT20* deletion strain (Fig. 5B). Although transcription of *ARG4* is unaffected by mutations in NuA4 subunits, both *HIS4* and *ARG1* transcription are NuA4 dependent, showing that NuA4 functions in a gene-specific manner at Gcn4-dependent genes. Reduced transcription was observed for six *TRA1* mutants (Δ2, Δ5, Δ17, Δ24, Δ32, and Δ41) ranging from 40 to 60% of wild-type levels (Fig. 6D to F). Interestingly, the transcription results for the Gcn4- and Rap1-dependent genes were very similar, suggesting that these *TRA1* mutations cause similar transcriptional activation defects at both SAGA and NuA4-dependent genes.

To determine the cause of these defects, we used ChIP to measure cross-linking of Gcn4 and Pol II at *HIS4*. Under activated conditions, Gcn4 cross-linking to the *HIS4* promoter was unaltered in any of the *TRA1* mutant strains, and Pol II cross-linking correlated well with mRNA levels (Fig. 7E and F). Next, we measured the levels of SAGA recruited to the activated *HIS4* promoter by ChIP of Tra1 and the SAGA core subunit Spt7. Four *TRA1* mutants showed significant defects in SAGA recruitment at *HIS4* (deletions Δ2, Δ5, Δ17, and Δ41) (Fig. 7G and H). Three of these *TRA1* mutants also showed reduced NuA4 recruitment in Rap1-dependent transcription (Δ2, Δ5, and Δ17), suggesting that Rap1 (and/or other activators of ribosomal protein gene transcription) and Gcn4 target overlapping regions of Tra1 to recruit SAGA and NuA4 (Fig. 7C and G).

The final group tested included the Gal4- and SAGA-dependent genes *GAL1*, *GAL7*, and *GAL3*. Deletion of *SPT20* severely reduced activated mRNA levels of all these Gal4-dependent genes, consistent with several studies that showed that SAGA is an essential coactivator for these genes (Fig. 5C). In contrast, deletions of NuA4 subunits *EAF1* and *YNG2* reduced *GAL3* transcription by more than 2-fold, while *GAL1* and *GAL7* transcription remained relatively unchanged. Thus, like the Gcn4-dependent genes, Gal4-activated genes are dependent on SAGA and differentially dependent on NuA4 for their transcription.

The strongest transcription defects among the Gal4-dependent genes were observed for *TRA1* mutants Δ24, Δ32, and Δ41, while the remaining Tra1 mutants showed near-wild-type or only slightly reduced mRNA levels (Fig. 6G to I). Pol II cross-linking at the *GAL1* promoter correlated well with transcription levels for all mutants tested, while Gal4 cross-linking remained relatively unchanged, indicating that transcription defects occur after activation but before transcription initiation (Fig. 7I and J). Cross-linking of the SAGA subunits Tra1 and Spt7 at *GAL1* remained within 25% of the wild-type level for each of the Tra1 mutants, with the exception of Tra1 mutant Δ24, where cross-linking was reduced by 40% (Fig. 7K and L). Thus, Δ24 may disrupt a region of Tra1 that is important for recruitment of SAGA that is unique to the Gal4 activator. Furthermore, these results are consistent with a model where Gal4 and Gcn4 target different regions of Tra1, since the Tra1 mutants defective in recruitment by Gcn4 (Δ2, Δ5, and Δ17) show little or no defect in SAGA recruitment to the *GAL1* promoter.

To complement the ChIP assays, we used GST pulldown assays to test whether *TRA1* deletion mutations with recruitment defects are defective in activator binding. A GST-tagged fusion protein containing the two Gcn4 activation domains (residues 1 to 134) was mixed with Flag-Tra1, partially purified from whole-cell extracts, and the amount of Flag-Tra1 that

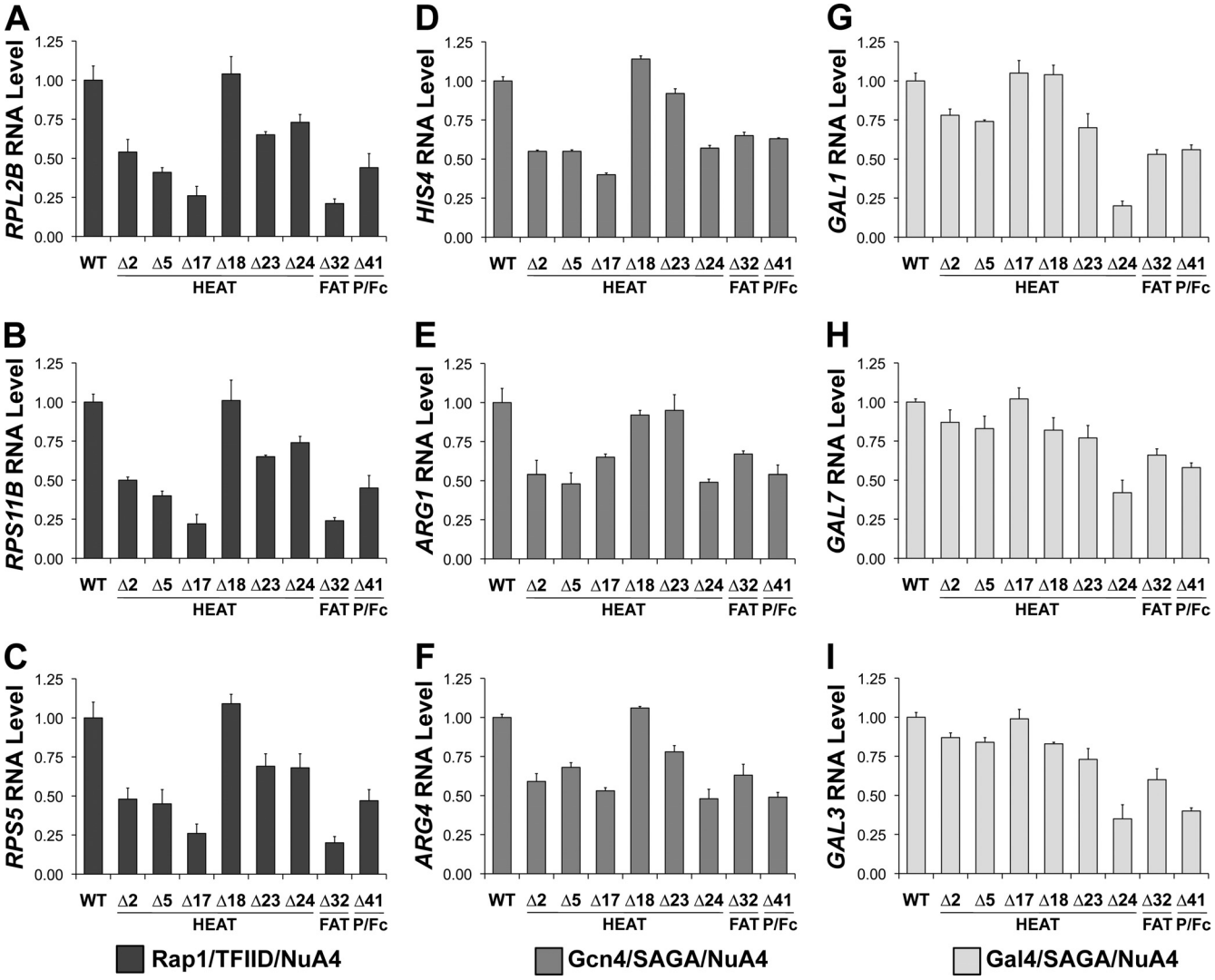

FIG. 6. Effect of *TRA1* mutations on transcription. Strains containing either wild-type *TRA1* or the indicted *TRA1* deletions were grown under conditions that induce Rap1-dependent genes (A to C), Gcn4-dependent genes (D to F), or Gal4-dependent genes (G to I). Total cellular RNA was prepared from these cells and quantitated by RT-qPCR, and results are represented relative to the wild-type value set at 1.0. Brackets below the *TRA1* mutant labels indicate the domain(s) disrupted by the deletion. P/Fc, junction between PI3K C-terminal lobe and FATC domains. Experiments were performed in biological triplicate, and errors bars represent standard deviations.

coprecipitates with GST-Gcn4 was determined. Compared to binding GST alone, each of the *TRA1* deletion mutants copurified with GST-Gcn4 to various degrees (Fig. 8A and B). *TRA1* deletion mutant Δ32 bound to GST-Gcn4 at near-wild-type levels, consistent with little or no defect in SAGA and NuA4 recruitment. The remaining *TRA1* deletion mutants reduced activator binding activity, ranging from 50 to 25% of wild-type levels. These results are consistent with the coactivator recruitment defects detected in these mutants, indicating that the reductions in SAGA and NuA4 recruitment *in vivo* are the direct result of a defect in activator binding.

Regions of Tra1 important for coactivator-mediated histone acetylation. *TRA1* deletions Δ24, Δ32, and Δ41 showed near-wild-type coactivator cross-linking at some promoters but low levels of activated transcription, suggesting a defect downstream of coactivator recruitment. Tra1 deletion mutant Δ32 exhibits the clearest postrecruitment defect that is neither activator nor coactivator specific, as it is observed at *RPL2B*, *HIS4*, and *GAL1*. A common postrecruitment function shared by SAGA and NuA4 is histone acetylation, an important step in the transcription activation process. H3 lysine 9 (H3K9Ac) and H4 lysine 8 (H4K8Ac) acetylation levels, which correlate well with transcription activation, were examined at the *RPL2B*, *HIS4*, and *GAL1* promoters in five *TRA1* deletion mutants: Δ5, Δ17, Δ24, Δ32, and Δ41.

We monitored NuA4-dependent H4 acetylation levels at the *RPL2B* promoter and SAGA-dependent H3 acetylation levels at the *HIS4* and *GAL1* promoters. At the *RPL2B* promoter, H4 acetylation levels were reduced by 50 to 70% in all mutants tested (Fig. 9A, dark gray bars). Similarly, H3 acetylation levels at the *HIS4* promoter showed decreased acetylation in each of the *TRA1* deletion mutants (Fig. 9B, dark gray bars). In con-

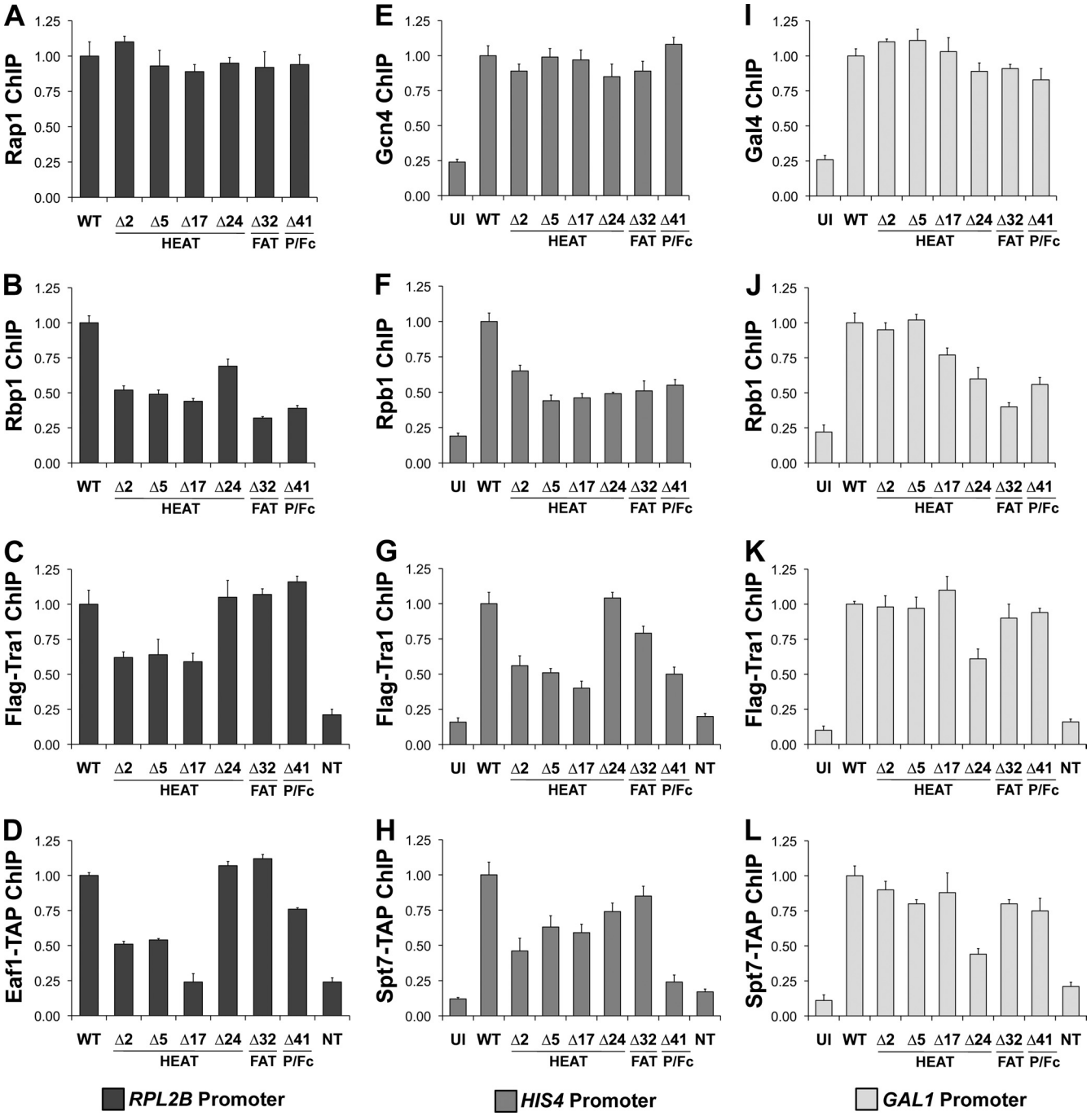

FIG. 7. Effect of *TRA1* mutations on recruitment of SAGA and NuA4 to promoters. Strains were grown as described for Fig. 6, cross-linked, and analyzed by ChIP: activator (A, E, and I), Rpb1 (B, F, and J), Flag-Tra1 (C, G, and K), Eaf1-TAP (D), and Spt7-TAP (H and L). ChIP results are represented relative to the wild-type value, set at 1.0. Different promoters analyzed by RT-qPCR are indicated. UI, not induced; NT, no epitope tag. Brackets below the *TRA1* mutant labels indicate the domain(s) disrupted by the deletion. P/Fc, junction between PI3K C-terminal lobe and FATc domains. Experiments were performed in biological triplicate, and error bars represent standard deviations.

trast, at the *GAL1* promoter, *TRA1* mutants Δ5 and Δ17 retained near-wild-type H3 acetylation levels, while *TRA1* mutants Δ24, Δ32, and Δ41 were decreased by between 40 and 60%, respectively (Fig. 9C, dark gray bars). These acetylation defects could be caused either by reduced activity of the HAT modules or by destabilization of the association of the HAT modules with SAGA and NuA4. *RPL2B*, *HIS4*, and *GAL1* transcription are all sensitive to loss of Gcn5, with transcription reduced by 50% or more when *GCN5* is deleted (Fig. 9D). Likewise, *RPL2B* and *HIS4* transcription is reduced by 50% or more in a conditional *ESA1* mutant when grown at 37°C (Fig. 9E).

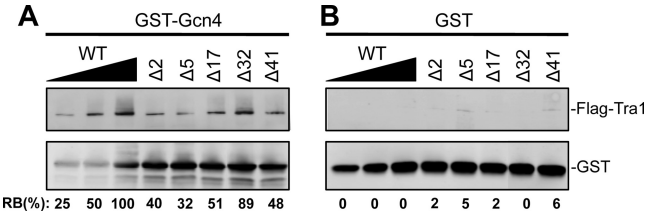

FIG. 8. *TRA1* mutations affect the binding of SAGA and NuA4 complexes to GST-Gcn4 fusion protein. Equivalent amounts of purified Flag-Tra1 coactivator complex were mixed and incubated with glutathione beads bound to GST-Gcn4 1–134 (A) or GST alone (B). Bound fractions were analyzed by Western blotting with antibodies against Flag and GST. Relative binding values (RB) represent the percentage of the Flag-Tra1 mutant retained relative to wild-type Flag-Tra1.

ChIP was used to measure recruitment of the HAT subunits Gcn5 and Esa1 to the *RPL2B*, *HIS4*, and *GAL1* promoters. For most *TRA1* mutants, defects in H3 and H4 acetylation correlated well with defects in HAT recruitment (Fig. 9A to C). A striking exception to this trend was *TRA1* mutant Δ32, in which Esa1 or Gcn5 cross-linking was near the wild-type level at *RPL2B*, *HIS4*, and *GAL1*, while H3 and H4 acetylation was reduced to 30 to 40% of the wild-type level. This suggests that deletion Δ32, located within the FAT domain, disrupts the HAT activity of both SAGA and NuA4. In contrast, the reduced HAT cross-linking in *TRA1* mutants Δ24 and Δ41 does not correlate well with the near-normal Tra1 levels detected at *RPL2B* and *HIS4*, suggesting that these Tra1 mutations destabilize association of the HAT modules.

The HAT module of SAGA consists of three subunits: Ada2, Ada3, and Gcn5 (6, 31). To determine whether SAGA HAT module integrity is disrupted for *TRA1* mutants Δ24, Δ32, and Δ41, we immunoprecipitated Flag-Tra1 and assessed the levels of the HAT components that coprecipitate with Flag-Tra1 by Western blotting (Fig. 9F). *TRA1* mutant Δ24 showed clear reductions in Gcn5, Ada3, and Ada2 association (20%, 30%, and 50% of wild-type levels, respectively), while HAT module subunits remained at or near wild-type levels for *TRA1* mutants Δ32 and Δ41. To further examine HAT module stability, we immunoprecipitated Gcn5 and quantitated coprecipitation of the various Tra1 derivatives (Fig. 9G). In this experiment, equivalent amounts of Gcn5 were loaded to more easily compare the amounts of coprecipitating Tra1. A 2-fold reduction was observed in the amount of Tra1 Δ24 coprecipitating with Gcn5 (lanes 2 and 3). In contrast, Tra1 Δ41 showed only a slight decrease in coprecipitating Tra1 (75% of wild-type level) while Tra1 Δ32 showed no defect in Tra1-Gcn5 association. As expected, Ada2 and Ada3 associated normally with Gcn5 in all strains tested, as these three proteins interact independently of Tra1.

Finally, we tested HAT activity of the Flag-Tra1 purified complexes. Immunoprecipitates of Tra1 from wild-type or mutant strains were assayed for acetylation of recombinant H3 at residue K9 as a measure of intrinsic HAT activity (Fig. 9H). These assays used Flag-Tra1 immunoprecipitates similar to those in Fig. 9F and were normalized to utilize the same amounts of Flag-Tra1 in each HAT assay. As expected, we detected less H3K9 acetylation with *TRA1* mutant Δ24, consistent with a HAT module association defect (Fig. 9H, lane 3). However, HAT assays using Flag-Tra1 Δ32 and Δ41 complexes showed activity similar to that of wild-type Flag-Tra1 complexes. Our combined results show that *TRA1* mutant Δ24 affects association with the Gcn5 HAT module while the phenotypes of *TRA1* mutant Δ32 are clearly caused by a postrecruitment defect.

DISCUSSION

Tra1 and its human homolog TRRAP are key subunits of several conserved HAT complexes that are targeted to gene regulatory regions by transcription activators. In yeast, Tra1 is a component of the HAT complexes NuA4 and SAGA, which share no subunits other than Tra1. Although Tra1 and TRRAP directly contact activators, little is known of the additional roles of Tra1 within SAGA and NuA4 complexes. Here we identified other important and surprising functions for Tra1 within these coactivators that are listed in Table 1. In summary, we analyzed the sequence of Tra1 and identified regions important for cell viability, integrity of SAGA and NuA4 complexes, transcription activation, activator interaction, coactivator recruitment, and *in vivo* HAT activity. These findings suggest that the majority of the Tra1 acts as a protein scaffold for association with other SAGA and NuA4 subunits and that other distinct regions contribute to activator interaction and HAT activity.

Sequence analysis showed that Tra1 can be divided into five separate domains. Two of these domains (HEAT and FAT), comprising 86% of Tra1, are composed of short helical repeats. Tandem HEAT repeats are present in a wide variety of proteins involved in signaling and are a common protein-protein interaction motif (4). Structural studies showed that these arrays form an elongated superhelix and that, in some cases, proteins interact with these repeats by binding within the groove of the superhelix (30). Our analysis found that Tra1 and TRRAP have a remarkably similar repeat configuration despite their low sequence identity.

Based on this analysis, a series of *TRA1* mutations that eliminate 1 to 3 repeat motifs or disrupt other conserved domains were generated to identify the functional regions of Tra1. For such a large protein, much of which consists of repeated motifs, it was surprising that about two-thirds of the protein was essential for cell viability. We found that all of the lethal Tra1 mutations had the same biochemical phenotype: complete dissociation of Tra1 from other subunits of both NuA4 and SAGA. These assembly-defective mutations were found over wide regions of Tra1 and were located in all five conserved domains. Since no SAGA subunit other than Tra1 is essential for viability, it is likely that the lethality of these mutations is due to disruption of NuA4 function, since the NuA4 subunit Esa1 is essential. Mutagenesis of putative surface residues within this domain suggested that only a small surface of the PI3K-like domain is critical for function, and it may play a structural role in coactivator assembly.

It was remarkable that all of the lethal *TRA1* mutations disrupted interactions with both NuA4 and SAGA subunits, suggesting that overlapping regions of Tra1 interact with subunits of both SAGA and NuA4 that have no apparent sequence similarity. Some of these mutations likely eliminated

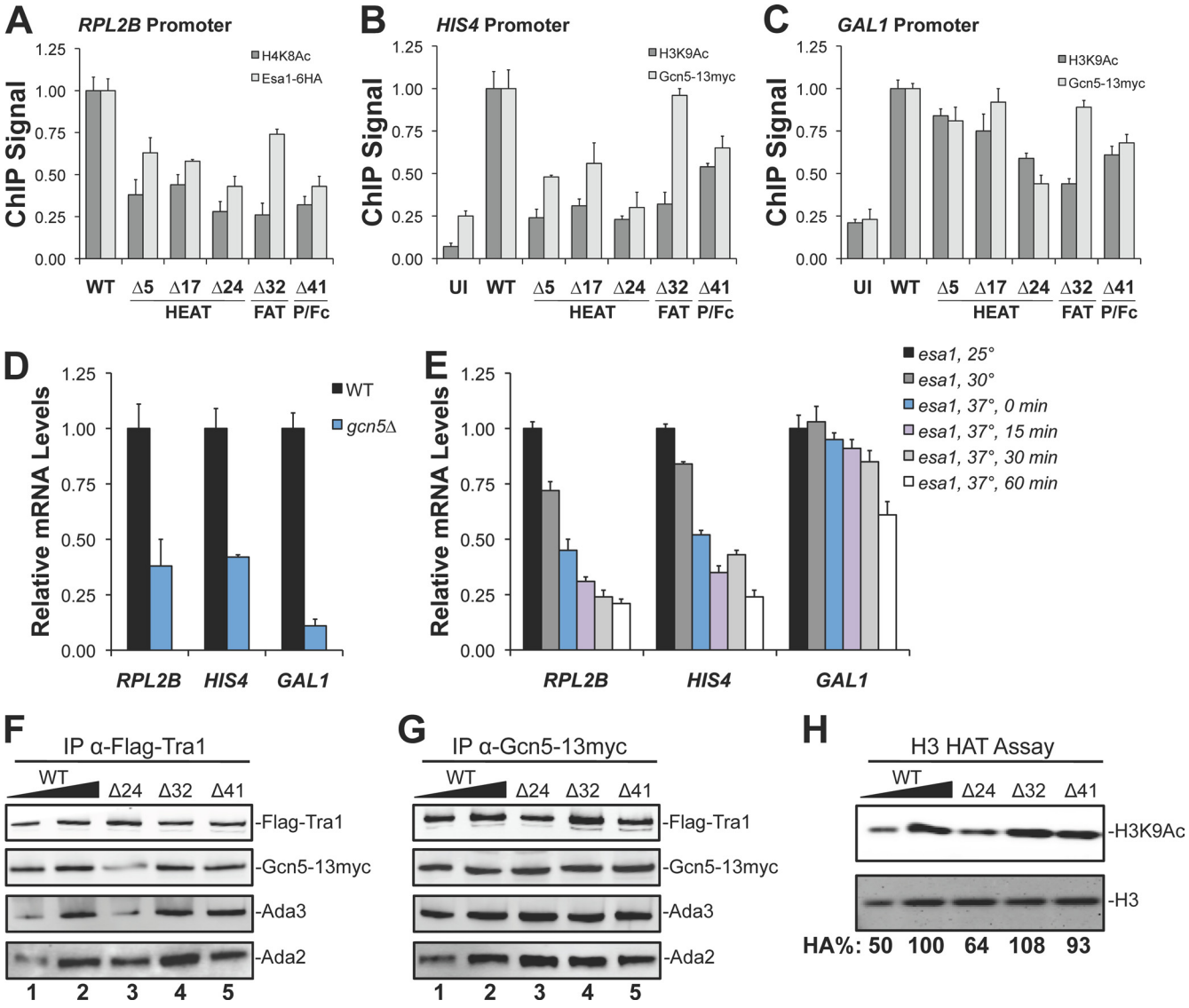

FIG. 9. Effect of *TRA1* deletions on HAT subunit recruitment, histone acetylation levels, and HAT module integrity. (A to C) Strains were grown as described for Fig. 4 and analyzed by ChIP at the indicated genes. Shown are the ChIP results obtained with Esa1-6HA and H4K8Ac (A) or Gcn5-13Myc and H3K9Ac (B and C). Histone ChIP results are shown as the ratio of acetylated to total H3 or H4 relative to the wild-type value, set at 1.0. HAT ChIP results are shown relative to the wild-type value, set at 1.0. UI, not induced. Brackets below the *TRA1* mutant labels indicate the domain(s) disrupted by the deletion. P/Fc, junction between PI3K C-terminal lobe and FATc domains. (D) Relative mRNA levels from a *gcn5*Δ strain grown at 30°C. (E) Relative mRNA levels from an *esa1* temperature-sensitive mutant strain grown at 30°C or shifted to 37°C for the indicated times before gene induction. Experiments were performed in biological duplicate, and errors bars represent standard deviations. (F and G) Western analysis of immunoprecipitated Flag-Tra1 (F) and Gcn5-13myc (G) complexes. Amounts of the immunoprecipitate (IP) loaded were normalized to load equivalent amounts of Tra1 and Gcn5, respectively. Purified complexes were analyzed by Western blotting using the following antibodies: Flag, Myc, Ada2, and Ada3. (H) Histone H3 HAT activity of Flag-Tra1 purified complexes. Equivalent amounts of Flag-Tra1 purified complexes were incubated with free histone H3 and analyzed by Western blotting using antibodies against H3K9Ac. Coomassie blue staining was used as a loading control to assess total H3 levels in each reaction mixture. Relative HAT activity levels (HA) represent the percentages of the H3K9Ac acetylation levels relative to wild-type Flag-Tra1.

regions of Tra1 that directly interact with other coactivator subunits, although others may have disrupted coactivator integrity because of an indirect structural defect. Solenoid proteins such as Tra1 are very flexible compared to more rigid globular proteins, possibly allowing Tra1 to adapt distinct coactivator-specific conformations (44).

About one-third of the targeted *TRA1* mutations were not lethal, allowing us to probe the role of Tra1 in gene expression. We examined transcriptional defects at three types of genes: NuA4-dependent genes, SAGA-dependent genes, and genes dependent on both coactivators. We found that the nonlethal Tra1 mutations fell into three general classes: (i) defective recruitment to promoters, (ii) reduced stability of the SAGA and NuA4 HAT module, and (iii) normal recruitment of Tra1-associated subunits but reduced HAT activity *in vivo*.

We found that the *TRA1* mutations with reduced recruit-

TABLE 1. Summary of the biochemical phenotypes observed for the *TRA1* deletion mutants generated from this study

Biochemical phenotype	*TRA1* deletion mutant(s)
Coactivator complex assembly defect	Δ6, Δ8-16, Δ19-20, Δ26-31, Δ33-40, Δ42
Transcription activation defect	Δ2,[a] Δ5,[a] Δ17,[a] Δ24, Δ32, Δ41
Coactivator recruitment defect	Δ2,[a] Δ5,[a] Δ17,[a] Δ24,[c] Δ41[d]
HAT module association defect	Δ24, Δ41
HAT module acetylation defect	Δ32
Post-coactivator recruitment defect	Δ24,[a] Δ32, Δ41[b]

[a] Specific for Rap1- and Gcn4-dependent genes.
[b] Specific for Rap1- and Gal4-dependent genes.
[c] Specific for Gal4-dependent genes.
[d] Specific for Gcn4-dependent genes.

ment at Rap1- and Gcn4-dependent genes largely overlapped (Δ2, Δ5, and Δ17), lying within the N-terminal region of the HEAT domain. These results suggest that Gcn4 and Rap1 (and/or other activators of ribosomal protein gene transcription) target identical regions of Tra1. These recruitment-defective *TRA1* mutations caused identical defects in both SAGA and NuA4, showing that these repeat regions play similar roles in activator recruitment of both complexes. Direct binding assays using whole-cell extracts showed that Tra1 containing these mutations bound less well to immobilized Gcn4 activator, confirming the *in vivo* phenotype. In contrast, none of these *TRA1* mutations was significantly defective for recruitment of SAGA or NuA4 to Gal4-regulated genes. This suggests that Gal4 targets distinct or additional regions of Tra1. For example, Gal4 could target more regions of Tra1 than could Gcn4, so that deletion of only one or two activator binding sites has little phenotype. A previously reported temperature-sensitive Tra1 allele with multiple mutations in the FAT domain was also defective in Gcn4 activator interaction (17). This result, combined with our new findings, suggests that activators target multiple regions of Tra1. Multiple contacts of activators with coactivator complexes may be a general mechanism for activator recruitment. For example, the Mediator subunit Gal11/Med15 contains at least three relatively low affinity Gcn4 activator binding domains that function additively (33, 40, 67), while SWI/SNF contains two activator binding domains with one on each of two subunits (71).

The second class of nonlethal *TRA1* mutations showed near-normal Tra1 cross-linking in ChIP assays but lower levels of acetylated H3/H4 at SAGA- and NuA4-dependent genes. The most striking example is mutation Δ32, located within the FAT domain, which shows a strong difference between cross-linking of the HAT subunits and the level of acetylated H3/H4 *in vivo*. This mutation shows that Tra1 somehow influences either specificity or catalytic activity of the HAT subunit without disrupting the association of HAT module components Ada2 and Ada3. It was previously found that several mutations within the PI3K-like domain of Tra1 showed *in vivo* defects in histone acetylation but no defect in Tra1 recruitment (61). Our initial experiments show that SAGA containing *TRA1* Δ32 has normal activity in acetylating recombinant H3 at residue K9. Future studies will be required to determine whether the *in vivo* acetylation defect is direct or indirect and, if direct, whether it is the result of reduced acetylation activity with nucleosomal substrates.

The final class of *TRA1* mutations shows near-normal Tra1 recruitment but reduced promoter-cross-linking of Esa1 and Gcn5. An example of this phenotype is *TRA1* mutant Δ24, which shows reduced HAT cross-linking at both the *RPL2B* and *HIS4* promoters and acts by specifically destabilizing the SAGA HAT module. *TRA1* mutant Δ41 has a related but more complex phenotype with reduced *in vivo* HAT cross-linking but no apparent defect in association of Gcn5 HAT module components. Determining the biochemical defect in this mutant must await further study. However, from our combined studies, it is clear that Tra1 plays an important role in HAT module association and *in vivo* HAT activity.

Since the overall domain and repeat architectures of Tra1 and TRRAP are nearly identical, our findings on the functional regions of Tra1 will likely correspond to similar biochemical properties of TRRAP within its coactivator complexes. This similarity appears to be a common characteristic of PIKK protein family members when homologs in different organisms are compared (43). For example, the domain architectures of human and yeast TOR, a PIKK protein family member, differ only by the absence or presence of two HEAT repeats in the HEAT domain, whereas the remaining repeat and domain architectures are the same (43). Future studies to examine the role of each Tra1 domain in protein-protein interactions with SAGA and NuA4 components as well as with activators should reveal how these two divergent coactivator complexes use a common subunit for similar biochemical functions.

ACKNOWLEDGMENTS

We thank Jerry Workman (Stowers Institute) for kindly providing Tra1, members of the Hahn Laboratory and Ted Young (University of Washington) for critical discussion throughout the course of this work, Beth Moorefield and Ivanka Kamenova for critical review of the manuscript, and members of the Tsuikiyama lab (FHCRC) and Biggins lab (FHCRC) for providing yeast tagging plasmids and equipment.

This work was supported by T32 CA09657 to B.A.K. and grant RO1 GM075114 to S.H.

REFERENCES

1. **Abraham, R. T.** 1996. Phosphatidylinositol 3-kinase related kinases. Curr. Opin. Immunol. **8:**412–418.
2. **Abraham, R. T.** 2004. PI 3-kinase related kinases: 'big' players in stress-induced signaling pathways. DNA Repair (Amst.) **3:**883–887.
3. **Allard, S., et al.** 1999. NuA4, an essential transcription adaptor/histone H4 acetyltransferase complex containing Esa1p and the ATM-related cofactor Tra1p. EMBO J. **18:**5108–5119.
4. **Andrade, M. A., C. Petosa, S. I. O'Donoghue, C. W. Muller, and P. Bork.** 2001. Comparison of ARM and HEAT protein repeats. J. Mol. Biol. **309:**1–18.
5. **Andrade, M. A., C. P. Ponting, T. J. Gibson, and P. Bork.** 2000. Homology-based method for identification of protein repeats using statistical significance estimates. J. Mol. Biol. **298:**521–537.
6. **Auger, A., et al.** 2008. Eaf1 is the platform for NuA4 molecular assembly that evolutionarily links chromatin acetylation to ATP-dependent exchange of histone H2A variants. Mol. Cell. Biol. **28:**2257–2270.
7. **Berman, H. M., et al.** 2000. The Protein Data Bank. Nucleic Acids Res. **28:**235–242.
8. **Bhaumik, S. R., T. Raha, D. P. Aiello, and M. R. Green.** 2004. In vivo target of a transcriptional activator revealed by fluorescence resonance energy transfer. Genes Dev. **18:**333–343.
9. **Biegert, A., and J. Soding.** 2008. De novo identification of highly diverged protein repeats by probabilistic consistency. Bioinformatics **24:**807–814.
10. **Bird, A. W., et al.** 2002. Acetylation of histone H4 by Esa1 is required for DNA double-strand break repair. Nature **419:**411–415.
11. **Borghouts, C., A. Benguria, J. Wawryn, and S. M. Jazwinski.** 2004. Rtg2 protein links metabolism and genome stability in yeast longevity. Genetics **166:**765–777.
12. **Bosotti, R., A. Isacchi, and E. L. Sonnhammer.** 2000. FAT: a novel domain in PIK-related kinases. Trends Biochem. Sci. **25:**225–227.

13. **Bouchard, C., et al.** 2001. Regulation of cyclin D2 gene expression by the Myc/Max/Mad network: Myc-dependent TRRAP recruitment and histone acetylation at the cyclin D2 promoter. Genes Dev. **15:**2042–2047.
14. **Brachmann, C. B., et al.** 1998. Designer deletion strains derived from Saccharomyces cerevisiae S288C: a useful set of strains and plasmids for PCR-mediated gene disruption and other applications. Yeast **14:**115–132.
15. **Brand, M., K. Yamamoto, A. Staub, and L. Tora.** 1999. Identification of TATA-binding protein-free TAFII-containing complex subunits suggests a role in nucleosome acetylation and signal transduction. J. Biol. Chem. **274:**18285–18289.
16. **Brewerton, S. C., A. S. Dore, A. C. Drake, K. K. Leuther, and T. L. Blundell.** 2004. Structural analysis of DNA-PKcs: modelling of the repeat units and insights into the detailed molecular architecture. J. Struct. Biol. **145:**295–306.
17. **Brown, C. E., et al.** 2001. Recruitment of HAT complexes by direct activator interactions with the ATM-related Tra1 subunit. Science **292:**2333–2337.
18. **Bystroff, C., and A. Krogh.** 2008. Hidden Markov Models for prediction of protein features. Methods Mol. Biol. **413:**173–198.
19. **Charles, N. A., and E. C. Holland.** 2010. TRRAP and the maintenance of stemness in gliomas. Cell Stem Cell **6:**6–7.
20. **Dames, S. A., J. M. Mulet, K. Rathgeb-Szabo, M. N. Hall, and S. Grzesiek.** 2005. The solution structure of the FATC domain of the protein kinase target of rapamycin suggests a role for redox-dependent structural and cellular stability. J. Biol. Chem. **280:**20558–20564.
21. **DeLano, W. L.** 2008. The PyMOL molecular graphics system. DeLano Scientific LLC, Palo Alto, CA.
22. **Deleu, L., S. Shellard, K. Alevizopoulos, B. Amati, and H. Land.** 2001. Recruitment of TRRAP required for oncogenic transformation by E1A. Oncogene **20:**8270–8275.
23. **Downs, J. A., et al.** 2004. Binding of chromatin-modifying activities to phosphorylated histone H2A at DNA damage sites. Mol. Cell **16:**979–990.
24. **Durant, M., and B. F. Pugh.** 2007. NuA4-directed chromatin transactions throughout the *Saccharomyces cerevisiae* genome. Mol. Cell. Biol. **27:**5327–5335.
25. **Fishburn, J., N. Mohibullah, and S. Hahn.** 2005. Function of a eukaryotic transcription activator during the transcription cycle. Mol. Cell **18:**369–378.
26. **Frangioni, J. V., and B. G. Neel.** 1993. Solubilization and purification of enzymatically active glutathione S-transferase (pGEX) fusion proteins. Anal. Biochem. **210:**179–187.
27. **Galarneau, L., et al.** 2000. Multiple links between the NuA4 histone acetyltransferase complex and epigenetic control of transcription. Mol. Cell **5:**927–937.
28. **Ginsburg, D. S., C. K. Govind, and A. G. Hinnebusch.** 2009. NuA4 lysine acetyltransferase Esa1 is targeted to coding regions and stimulates transcription elongation with Gcn5. Mol. Cell. Biol. **29:**6473–6487.
29. **Govind, C. K., F. Zhang, H. Qiu, K. Hofmeyer, and A. G. Hinnebusch.** 2007. Gcn5 promotes acetylation, eviction, and methylation of nucleosomes in transcribed coding regions. Mol. Cell **25:**31–42.
30. **Graham, T. A., C. Weaver, F. Mao, D. Kimelman, and W. Xu.** 2000. Crystal structure of a beta-catenin/Tcf complex. Cell **103:**885–896.
31. **Grant, P. A., et al.** 1997. Yeast Gcn5 functions in two multisubunit complexes to acetylate nucleosomal histones: characterization of an Ada complex and the SAGA (Spt/Ada) complex. Genes Dev. **11:**1640–1650.
32. **Grant, P. A., D. Schieltz, M. G. Pray-Grant, J. R. Yates III, and J. L. Workman.** 1998. The ATM-related cofactor Tra1 is a component of the purified SAGA complex. Mol. Cell **2:**863–867.
33. **Herbig, E., et al.** 2010. Mechanism of mediator recruitment by tandem Gcn4 activation domains and three Gal11 activator-binding domains. Mol. Cell. Biol. **30:**2376–2390.
34. **Herceg, Z., et al.** 2001. Disruption of Trrap causes early embryonic lethality and defects in cell cycle progression. Nat. Genet. **29:**206–211.
35. **Herceg, Z., et al.** 2003. Genome-wide analysis of gene expression regulated by the HAT cofactor Trrap in conditional knockout cells. Nucleic Acids Res. **31:**7011–7023.
36. **Hoke, S. M., et al.** 2010. Mutational analysis of the C-terminal FATC domain of *Saccharomyces cerevisiae* Tra1. Curr. Genet. **56:**447–465.
37. **Huisinga, K. L., and B. F. Pugh.** 2004. A genome-wide housekeeping role for TFIID and a highly regulated stress-related role for SAGA in Saccharomyces cerevisiae. Mol. Cell **13:**573–585.
38. **Hunter, T.** 1995. When is a lipid kinase not a lipid kinase? When it is a protein kinase. Cell **83:**1–4.
39. **Ikura, T., et al.** 2000. Involvement of the TIP60 histone acetylase complex in DNA repair and apoptosis. Cell **102:**463–473.
40. **Jedidi, I., et al.** 2010. Activator Gcn4 employs multiple segments of Med15/Gal11, including the KIX domain, to recruit mediator to target genes in vivo. J. Biol. Chem. **285:**2438–2455.
41. **Jiang, X., Y. Sun, S. Chen, K. Roy, and B. D. Price.** 2006. The FATC domains of PIKK proteins are functionally equivalent and participate in the Tip60-dependent activation of DNA-PKcs and ATM. J. Biol. Chem. **281:**15741–15746.
42. **Karpenahalli, M. R., A. N. Lupas, and J. Soding.** 2007. TPRpred: a tool for prediction of TPR-, PPR- and SEL1-like repeats from protein sequences. BMC Bioinformatics **8:**2.
43. **Knutson, B. A.** 2010. Insights into the domain and repeat architecture of target of rapamycin. J. Struct. Biol. **170:**354–363.
44. **Kobe, B., and A. V. Kajava.** 2000. When protein folding is simplified to protein coiling: the continuum of solenoid protein structures. Trends Biochem. Sci. **25:**509–515.
45. **Komeili, A., K. P. Wedaman, E. K. O'Shea, and T. Powers.** 2000. Mechanism of metabolic control. Target of rapamycin signaling links nitrogen quality to the activity of the Rtg1 and Rtg3 transcription factors. J. Cell Biol. **151:**863–878.
46. **Kulesza, C. A., et al.** 2002. Adenovirus E1A requires the yeast SAGA histone acetyltransferase complex and associates with SAGA components Gcn5 and Tra1. Oncogene **21:**1411–1422.
47. **Kuninger, D., J. Lundblad, A. Semirale, and P. Rotwein.** 2007. A non-isotopic in vitro assay for histone acetylation. J. Biotechnol. **131:**253–260.
48. **Lang, S. E., S. B. McMahon, M. D. Cole, and P. Hearing.** 2001. E2F transcriptional activation requires TRRAP and GCN5 cofactors. J. Biol. Chem. **276:**32627–32634.
49. **Laprade, L., D. Rose, and F. Winston.** 2007. Characterization of new Spt3 and TATA-binding protein mutants of *Saccharomyces cerevisiae*: Spt3 TBP allele-specific interactions and bypass of Spt8. Genetics **177:**2007–2017.
50. **Lee, T. I., et al.** 2000. Redundant roles for the TFIID and SAGA complexes in global transcription. Nature **405:**701–704.
51. **Le Masson, I., et al.** 2003. Yaf9, a novel NuA4 histone acetyltransferase subunit, is required for the cellular response to spindle stress in yeast. Mol. Cell. Biol. **23:**6086–6102.
52. **Leone, M., et al.** 2006. The FRB domain of mTOR: NMR solution structure and inhibitor design. Biochemistry **45:**10294–10302.
53. **Lindstrom, K. C., J. C. Vary, Jr., M. R. Parthun, J. Delrow, and T. Tsukiyama.** 2006. Isw1 functions in parallel with the NuA4 and Swr1 complexes in stress-induced gene repression. Mol. Cell. Biol. **26:**6117–6129.
54. **Madison, J. M., and F. Winston.** 1997. Evidence that Spt3 functionally interacts with Mot1, TFIIA, and TATA-binding protein to confer promoter-specific transcriptional control in *Saccharomyces cerevisiae*. Mol. Cell. Biol. **17:**287–295.
55. **Martinez, E., T. K. Kundu, J. Fu, and R. G. Roeder.** 1998. A human SPT3-TAFII31-GCN5-L acetylase complex distinct from transcription factor IID. J. Biol. Chem. **273:**23781–23785.
56. **McMahon, S. B., H. A. Van Buskirk, K. A. Dugan, T. D. Copeland, and M. D. Cole.** 1998. The novel ATM-related protein TRRAP is an essential cofactor for the c-Myc and E2F oncoproteins. Cell **94:**363–374.
57. **McMahon, S. B., M. A. Wood, and M. D. Cole.** 2000. The essential cofactor TRRAP recruits the histone acetyltransferase hGCN5 to c-Myc. Mol. Cell. Biol. **20:**556–562.
58. **Mencia, M., Z. Moqtaderi, J. V. Geisberg, L. Kuras, and K. Struhl.** 2002. Activator-specific recruitment of TFIID and regulation of ribosomal protein genes in yeast. Mol. Cell **9:**823–833.
59. **Mitchell, L., et al.** 2008. Functional dissection of the NuA4 histone acetyltransferase reveals its role as a genetic hub and that Eaf1 is essential for complex integrity. Mol. Cell. Biol. **28:**2244–2256.
60. **Mohibullah, N., and S. Hahn.** 2008. Site-specific cross-linking of TBP in vivo and in vitro reveals a direct functional interaction with the SAGA subunit Spt3. Genes Dev. **22:**2994–3006.
61. **Mutiu, A. I., et al.** 2007. Structure/function analysis of the phosphatidylinositol-3-kinase domain of yeast tra1. Genetics **177:**151–166.
62. **Nelson, J. D., O. Denisenko, and K. Bomsztyk.** 2006. Protocol for the fast chromatin immunoprecipitation (ChIP) method. Nat. Protoc. **1:**179–185.
63. **Nelson, J. D., O. Denisenko, P. Sova, and K. Bomsztyk.** 2006. Fast chromatin immunoprecipitation assay. Nucleic Acids Res. **34:**e2.
64. **Nourani, A., R. T. Utley, S. Allard, and J. Cote.** 2004. Recruitment of the NuA4 complex poises the PHO5 promoter for chromatin remodeling and activation. EMBO J. **23:**2597–2607.
65. **Palidwor, G. A., et al.** 2009. Detection of alpha-rod protein repeats using a neural network and application to huntingtin. PLoS Comput. Biol. **5:**e1000304.
66. **Park, J., S. Kunjibettu, S. B. McMahon, and M. D. Cole.** 2001. The ATM-related domain of TRRAP is required for histone acetyltransferase recruitment and Myc-dependent oncogenesis. Genes Dev. **15:**1619–1624.
67. **Park, J. M., et al.** 2000. In vivo requirement of activator-specific binding targets of mediator. Mol. Cell. Biol. **20:**8709–8719.
68. **Pascual-Garcia, P., et al.** 2008. Sus1 is recruited to coding regions and functions during transcription elongation in association with SAGA and TREX2. Genes Dev. **22:**2811–2822.
69. **Perry, J., and N. Kleckner.** 2003. The ATRs, ATMs, and TORs are giant HEAT repeat proteins. Cell **112:**151–155.
70. **Pray-Grant, M. G., et al.** 2002. The novel SLIK histone acetyltransferase complex functions in the yeast retrograde response pathway. Mol. Cell. Biol. **22:**8774–8786.
71. **Prochasson, P., K. E. Neely, A. H. Hassan, B. Li, and J. L. Workman.** 2003. Targeting activity is required for SWI/SNF function in vivo and is accomplished through two partially redundant activator-interaction domains. Mol. Cell **12:**983–990.

72. **Reeves, W. M., and S. Hahn.** 2005. Targets of the Gal4 transcription activator in functional transcription complexes. Mol. Cell. Biol. **25:**9092–9102.
73. **Reid, J. L., V. R. Iyer, P. O. Brown, and K. Struhl.** 2000. Coordinate regulation of yeast ribosomal protein genes is associated with targeted recruitment of Esa1 histone acetylase. Mol. Cell **6:**1297–1307.
74. **Reid, J. L., Z. Moqtaderi, and K. Struhl.** 2004. Eaf3 regulates the global pattern of histone acetylation in *Saccharomyces cerevisiae*. Mol. Cell. Biol. **24:**757–764.
75. **Rodriguez-Navarro, S.** 2009. Insights into SAGA function during gene expression. EMBO Rep. **10:**843–850.
76. **Saleh, A., et al.** 1998. Tra1p is a component of the yeast Ada.Spt transcriptional regulatory complexes. J. Biol. Chem. **273:**26559–26565.
77. **Schultz, J., R. R. Copley, T. Doerks, C. P. Ponting, and P. Bork.** 2000. SMART: a web-based tool for the study of genetically mobile domains. Nucleic Acids Res. **28:**231–234.
78. **Schwede, T., J. Kopp, N. Guex, and M. C. Peitsch.** 2003. SWISS-MODEL: an automated protein homology-modeling server. Nucleic Acids Res. **31:**3381–3385.
79. **Sermwittayawong, D., and S. Tan.** 2006. SAGA binds TBP via its Spt8 subunit in competition with DNA: implications for TBP recruitment. EMBO J. **25:**3791–3800.
80. **Sigrist, C. J., et al.** 2002. PROSITE: a documented database using patterns and profiles as motif descriptors. Brief. Bioinform. **3:**265–274.
81. **Soding, J., A. Biegert, and A. N. Lupas.** 2005. The HHpred interactive server for protein homology detection and structure prediction. Nucleic Acids Res. **33:**W244–W248.
82. **Sonnhammer, E. L., S. R. Eddy, E. Birney, A. Bateman, and R. Durbin.** 1998. Pfam: multiple sequence alignments and HMM-profiles of protein domains. Nucleic Acids Res. **26:**320–322.
83. **Sterner, D. E., et al.** 1999. Functional organization of the yeast SAGA complex: distinct components involved in structural integrity, nucleosome acetylation, and TATA-binding protein interaction. Mol. Cell. Biol. **19:**86–98.
84. **Studier, F. W.** 2005. Protein production by auto-induction in high density shaking cultures. Protein Expr. Purif. **41:**207–234.
85. **Tamburini, B. A., and J. K. Tyler.** 2005. Localized histone acetylation and deacetylation triggered by the homologous recombination pathway of double-strand DNA repair. Mol. Cell. Biol. **25:**4903–4913.
86. **Templeton, G. W., and G. B. Moorhead.** 2005. The phosphoinositide-3-OH-kinase-related kinases of *Arabidopsis thaliana*. EMBO Rep. **6:**723–728.
87. **Weake, V. M., and J. L. Workman.** 2008. Histone ubiquitination: triggering gene activity. Mol. Cell **29:**653–663.
88. **Wu, P. Y., C. Ruhlmann, F. Winston, and P. Schultz.** 2004. Molecular architecture of the S. cerevisiae SAGA complex. Mol. Cell **15:**199–208.
89. **Wurdak, H., et al.** 2010. An RNAi screen identifies TRRAP as a regulator of brain tumor-initiating cell differentiation. Cell Stem Cell **6:**37–47.
90. **Wyce, A., et al.** 2007. H2B ubiquitylation acts as a barrier to Ctk1 nucleosomal recruitment prior to removal by Ubp8 within a SAGA-related complex. Mol. Cell **27:**275–288.